Kinetics of Relaxation from Rigor of Permeabilized Fast-Twitch Skeletal Fibers from the Rabbit Using a Novel Caged ATP and Apyrase
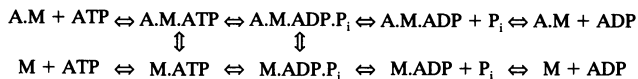
Hilary Thirlwell, John E. T. Corrie, Gordon P. Reid, David R. Trentham, and Michael A. Ferenczi

National Institute for Medical Research, Mill Hill, London NW7 1AA, United Kingdom

ABSTRACT　The complex time course of tension decay was investigated in fast-twitch permeabilized rabbit muscle fibers when they were relaxed from the rigor state using photochemical generation of ATP. A novel caged ATP compound, the P^3-3′,5′-dimethoxybenzoin ester of ATP (DMB-caged ATP), as well as the P^3-1-(2-nitrophenyl)ethyl ester of ATP (NPE-caged ATP), have been used. DMB-caged ATP photolyzes at least three orders of magnitude more rapidly than NPE-caged ATP. The role of ADP on relaxation kinetics from rigor was examined by using apyrase to remove ADP from the rigor muscle solutions. The presence of P_i-sensitive states was investigated from the effect of P_i on relaxation. Rigor tension was varied enabling the influence of tension on the relaxation to be examined. The time course of relaxation was faster with DMB-caged ATP compared with NPE-caged ATP for concentrations of ATP released by photolysis greater than 0.7 mM. Most of the complexity in the relaxation tension records was caused by ADP. In the absence of ADP, tension decayed monotonically after photochemical release of ATP in a process whose rate was unaffected by P_i. In the presence of ADP, relaxation was more complex and tension passed through a maximum. A model invoking cooperative interactions involving ADP-containing myosin heads provides a reasonable description of the data.

INTRODUCTION

Relaxation of muscle fibers from rigor can be initiated by flash photolysis of caged ATP, which enables the kinetics of the process to be studied. Here we describe the synthesis and use of a new caged ATP molecule, the P^3-3′,5′-dimethoxybenzoin ester of ATP (DMB-caged ATP) (Fig. 1) with the advantage over the P^3-1-(2-nitrophenyl)ethyl ester of ATP (NPE-caged ATP) of faster photolytic release of ATP ($>10^5$ s^{-1} as compared with 118 s^{-1} in rigor solution at 20°C in the absence of Ca^{2+}; Corrie et al., 1992; Goldman et al., 1984a). In the present study, DMB-caged ATP was used to test whether the rate of release of ATP from NPE-caged ATP limits the rate of relaxation from rigor.

A simple representation of the actomyosin ATPase mechanism in the cross-bridge cycle of fast-twitch skeletal muscle is shown in Scheme 1, in which A, M, and A.M represent actin, myosin, and actomyosin, respectively.

$$\text{A.M} + \text{ATP} \Leftrightarrow \text{A.M.ATP} \Leftrightarrow \text{A.M.ADP.P}_i \Leftrightarrow \text{A.M.ADP} + \text{P}_i \Leftrightarrow \text{A.M} + \text{ADP}$$
$$\Updownarrow \qquad\qquad \Updownarrow$$
$$\text{M} + \text{ATP} \;\Leftrightarrow\; \text{M.ATP} \;\Leftrightarrow\; \text{M.ADP.P}_i \;\Leftrightarrow\; \text{M.ADP} + \text{P}_i \;\Leftrightarrow\; \text{M} + \text{ADP}$$

Scheme 1

The top line represents attached cross-bridges, i.e., myosin cross-bridges attached or interacting with actin. The bottom line represents detached cross-bridges. The substrate for hydrolysis by myosin and actomyosin is MgATP, but is abbreviated here as ATP for clarity. In the absence of Ca^{2+} (the situation in the experiments reported here), the photogeneration of ATP might be expected to cause dissociation of A.M to A and M.ATP and the loss of rigor tension. This would be followed by myosin ATPase activity with essentially zero tension, but complex tension profiles are observed during the relaxation process.

A problem that has complicated the analysis of relaxation kinetics has been uncertainty about the ADP concentration in rigor muscle before photolytic release of ATP. Sleep and Burton (1990) have reported that apyrase can be added to skeletal muscle fibers in rigor and that this removes by hydrolysis any endogenous or contaminant ADP. Introduction of apyrase and introduction of known concentrations of ADP allows us to control ADP concentration and thereby extend earlier studies (Dantzig et al., 1991; Goldman et al., 1982, 1984a, b; Hibberd et al., 1984). It has also been shown that both P_i and the initial rigor tension markedly influence the kinetics of relaxation after photochemical release of ATP (Goldman et al., 1984a; Hibberd et al., 1985), but here also uncertainties exist in the levels of ADP present. These effects have been examined here at zero or known concentrations of ADP. Overall, the results show that ADP present initially has a profound effect on the relaxation kinetics. We have formulated a model of muscle relaxation from rigor based on earlier models, but incorporating cooperative properties only in initial states of cross-bridges containing bound ADP. Nucleotide-free cross-bridges behave noncooperatively in the model.

Some of the results have been presented as abstracts (Thirlwell et al., 1993a, b; Trentham et al., 1992).

MATERIALS AND METHODS

Chemistry

3′,5′-Dimethoxybenzoin phosphate (DMB-caged P_i) was prepared as its triethylammonium salt as described by Corrie and Trentham (1992). Anhydrous dimethylformamide was purchased from Aldrich (Milwaukee, WI)
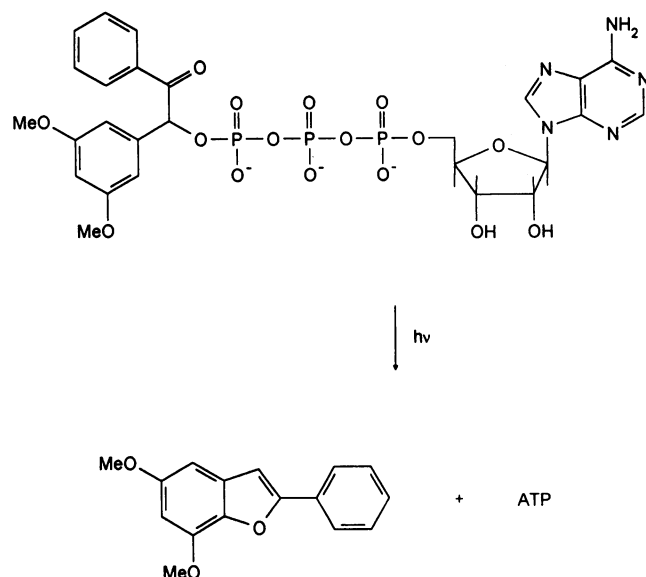
FIGURE 1   Structure and photolysis products of DMB-caged ATP.

and transferred under nitrogen by syringe. Anhydrous hexamethyl phosphoramide was prepared by vacuum distillation from calcium hydride. N,N'-Carbonyldiimidazole was from Lancaster Synthesis and was used only if its melting point was >110°C. Triethylammonium bicarbonate (TEAB) buffer was prepared by bubbling CO_2 into a 1 M solution of redistilled triethylamine in water at 4°C. Other reagents were the best available commercial grades and were used without further purification. ^{31}P NMR spectra were measured at 81 MHz using a Bruker WM 200 spectrometer for solutions in 20 mM Tris HCl plus 1 mM EDTA, pH 7.0, and referenced to 85% H_3PO_4.

NPE-caged ATP was synthesized by the method of Walker et al. (1989). HPLC analysis showed that ADP contamination was less than 0.1%.

DMB-caged ATP

ADP was purified in 1.0 mmol batches by chromatography on a column of DEAE-cellulose (2.2 × 45 cm) eluted with a linear gradient of TEAB, pH 7.5 (10–400 mM, total volume 2 l). Pooled fractions containing ADP were evaporated under reduced pressure and freed from residual buffer salts by repeated vacuum evaporation of methanol. A portion of the purified ADP triethylammonium salt (1.1 mmol) dissolved in water (50 ml) was treated with tri-n-octylamine (777 mg, 2.2 mmol) and rotary evaporated to dryness under vacuum. The residue was freed from traces of water by successive vacuum evaporation with pyridine (25 ml) and anhydrous dimethylformamide (4 × 25 ml) and finally re-dissolved in anhydrous dimethylformamide (10 ml).

In a second flask, a solution of the triethylammonium salt of 3',5'-dimethoxybenzoin phosphate (1.0 mmol) in water (50 ml) was treated with tri-n-octylamine (353 mg, 1.0 mmol) and evaporated under vacuum, and the residue was further evaporated with pyridine and dimethylformamide as above. A solution of N,N'-carbonyldiimidazole (810 mg, 5.0 mmol) in anhydrous dimethylformamide (25 ml) was added to the dried residue, and the mixture was stirred at room temperature for 4 h. Methanol (200 mg, 6.25 mmol) was added, the solution was stirred for an additional 45 min, and the solvent was evaporated under vacuum. The residue was re-dissolved in anhydrous dimethylformamide (10 ml) and added to the solution of ADP prepared above. A copious precipitate formed immediately, and the solvent was again evaporated under vacuum. Anhydrous hexamethyl phosphoramide (5–10 ml) was added, and the stoppered flask was shaken vigorously for 24 h, during which time the precipitate slowly dissolved to give a clear solution. Reverse phase HPLC analysis (Merck RP8 LichroCart column, Cat. No. 50832, with 25 mM KH_2PO_4 adjusted to pH 6.0 with 1 M KOH, plus 35% methanol v/v as mobile phase at 1.5 ml min^{-1}) indicated a 43%

yield of the required triphosphate. Retention times were 1.8, 2.95, and 5.1 min, respectively, for ADP, DMB-caged ATP, and DMB-phosphate.

The solution was diluted with water (200 ml), adjusted to pH 7.0, and chromatographed in two equal batches on a DEAE-cellulose column, as above, using a linear gradient of TEAB (10–500 mM, total volume 2 l). Column fractions were analyzed by reverse phase HPLC, and those fractions containing DMB-caged ATP were pooled, adjusted to pH 6.0, and split into two equal portions. In separate runs, each portion was pumped at 2.5 ml min^{-1} onto a preparative reverse phase HPLC column (2 × 30 cm; Waters C_{18} packing material, Cat. No. 20594) equilibrated in 5 mM potassium phosphate, pH 6.0. After loading, the same potassium phosphate buffer was pumped through the column until elution of ADP ceased. The mobile phase was then changed to distilled water (pH 5.0, presumably because of atmospheric CO_2), which eluted DMB-caged ATP once the conductivity of the eluent had dropped to that of distilled water. This protocol was adopted to avoid exposure of DMB-caged ATP to TEAB buffer during its final purification. During vacuum evaporation, TEAB buffer reaches at least pH 8.5, which promotes the spontaneous hydrolysis of DMB-caged ATP (see below). Pooled fractions containing DMB-caged ATP were evaporated at 1 mmHg and <35°C. The residue was re-dissolved in water (approximately 4 ml), and the concentration was determined by quantitative UV absorbance at 256 nm. The measured UV spectrum at pH 7.0 matched that obtained by summation of the individual spectra of ADP and 3',5'-dimethoxybenzoin phosphate. From these data, the calculated extinction coefficient of DMB-caged ATP is 25,600 M^{-1} cm^{-1} at 256 nm. The yield of DMB-caged ATP was 31% (based on DMB-phosphate), and contamination by ADP when freshly prepared was 1%. Aliquots of DMB-caged ATP were stored frozen in liquid nitrogen.

Spontaneous hydrolysis of DMB-caged ATP

Solutions of 2 mM DMB-caged ATP were prepared in each of the following buffer solutions: i) 10 mM K phosphate, pH 7.0; ii) 10 mM Na bicarbonate, pH 9.5. Solutions were incubated at 30°C, and aliquots were withdrawn at varying time intervals and rapidly frozen. AMP and ADP were determined by anion exchange HPLC (Whatman Partisphere SAX column, Cat. No. 4621–0505, with 0.25 M $NH_4H_2PO_4$ adjusted to pH 6.0 with 1 M NaOH, as mobile phase at 1.5 ml min^{-1}), and 3',5'-dimethoxybenzoin phosphate was determined by reverse phase HPLC (Waters μBondapak C_{18} column with 25 mM KH_2PO_4, adjusted to pH 6.0 with 1 M KOH, plus 30% methanol v/v as mobile phase at 1.5 ml min^{-1}). For each set of analyses, quantification was by means of a standard curve of peak heights against known masses of injected standards. Retention times on anion exchange were 1.4 and 2.2 min for AMP and ADP, respectively. DMB-caged ATP and DMB-phosphate co-eluted at 2.7 min in this mobile phase. On reverse phase, retention times were 6.4 and 12.6 min for DMB-caged ATP and DMB-phosphate, respectively.

Estimation of the extent of photolysis

Samples of solution taken from the experimental troughs were treated with 10.5 units ml^{-1} apyrase for 5 min at 4°C (see below; Molnar and Lorand, 1961) so that all ATP and ADP was hydrolyzed to AMP with little breakdown of AMP by the low AMPase activity of the enzyme preparation. The samples were then loaded on a Whatman Partisphere SAX HPLC column with 0.125 M $(NH_4)_2HPO_4$ (adjusted to pH 5.9 with concentrated HCl) plus 5% methanol as the mobile phase at a flow rate of 1.5 ml min^{-1}. The retention times for AMP and DMB-caged ATP were 80 and 120 s, respectively. The extent of photolysis was calculated by reference to pre-established calibration curves for the amplitude of the elution peaks observed by their absorbance at 260 nm.

Apyrase

ADP contamination was removed by means of apyrase obtained from Sigma Chemical Co. (A-6535, Grade VII; St. Louis, MO). The lyophilized powder was dissolved in 50 mM TES solution, pH 7.1 (~3 mg ml^{-1}), and quickly

frozen in 30 μl aliquots in liquid nitrogen. The enzyme was stored at $-80°C$ for no longer than 2 weeks. A fresh aliquot of enzyme was thawed on the day of each experiment. The activity of apyrase was assayed using ADP as a substrate and measuring P_i release by the method of Webb (1992). Note that the activity of the apyrase decreased significantly for each freezing/thawing of the stock solution.

Coupling of apyrase to Sepharose beads

In experiments where ADP was removed from experimental solutions and subsequently added (Fig. 3), apyrase was coupled to cyanogen bromide-activated Sepharose 4B beads of 90 μm diameter. The immobilized apyrase could be used to treat experimental solutions and then be removed by centrifugation; when required, known concentrations of ADP were added subsequently.

To prepare immobilized apyrase, 1 g of freeze-dried, CNBr-activated Sepharose 4B beads (Pharmacia LKB Biotechnology) was suspended in 10 ml of 1 mM HCl and the gel was washed for 15 min with 1 mM HCl on a sintered glass filter. 1.4 mg of apyrase was dissolved in 1 ml of a solution of 0.5 M NaCl and 0.1 M NaHCO$_3$ and dialysed overnight at 5°C in the same solution. Coupling to CNBr-activated beads was achieved following the manufacturer's instructions by adding 1 ml of CNBr-activated Sepharose gel to the apyrase solution, sealing it in a 20 ml vial, and rotating the mixture end over end for 1 h at room temperature. The gel was washed with 10 ml of the NaHCO$_3$ solution, and remaining active groups on the gel were blocked by 2 h incubation at room temperature with 1 ml of 0.1 M Tris-HCl, pH 8.0. Unbound apyrase was removed by three cycles of alternating 20 ml washes on a sintered glass filter using 0.5 M NaCl, 0.1 M Na acetate, pH 4.0, and 0.5 M NaCl, 0.1 M Tris-HCl, pH 8.0. The gel was resuspended in 1 ml of 50 mM TES buffer adjusted to pH 7.1 with KOH and stored for 2 days at 4°C.

The ADPase activity of the Sepharose-coupled apyrase was assayed by incubation with ADP for varying time periods. The mixture was centrifuged at 2000 rpm for 1 min to separate the resin, and a sample of the supernatant was assayed on a SAX column by monitoring the disappearance of the ADP peak in the HPLC elution. The anion exchange HPLC conditions were as for the analysis of DMB-caged ATP. The ADPase activity, at room temperature ($\sim20°C$), was at least 82.5 nmol min^{-1} ml^{-1} wet volume of the immobilized apyrase. To treat experimental caged ATP solutions, 50 μl of this stock was added to a 200 μl volume of 5 mM NPE-caged ATP and incubated for 30 min at room temperature to remove contaminating ADP.

Muscle fibers

Adult California Giant rabbits (Hylyne Rabbits Ltd., Lymm, Cheshire) were killed by inhalation of a rising concentration of CO$_2$. The psoas muscle was exposed ventrally and cooled rapidly in situ with crushed ice (Kawai et al.,

1993). Twelve to twenty small bundles of skeletal muscle fibers (0.2–1 mm ϕ, 3–5 cm long) were dissected from the psoas muscle and tied at rest length to wooden applicator sticks. The muscle cells in the bundles were permeabilized by a method based on Eastwood et al. (1979). The bundles were bathed for 2 h at 0°C in 250 ml of a solution containing 70 mM Na propionate, 8 mM Mg acetate, 5 mM K$_2$EGTA, 7 mM Na$_2$ATP, 6 mM imidazole, 10 μM phenylmethylsulfonyl fluoride, 50 mg l^{-1} trypsin inhibitor, 4 mg l^{-1} leupeptin. After 2, 4, and 12 h, the bundles were transferred to beakers containing 12.5, 25, and 50% glycerol, respectively, in the same solution. After 24 h, the bundles in 50% glycerol were transferred to $-18°C$ and used for a period of up to 6 weeks. Four- to eight-mm-long segments of single muscle fibers were dissected from the bundles on a cooled microscope stage and mounted by means of aluminium T-clips (Goldman and Simmons, 1984) to the apparatus. In most experiments, the ends of the muscle fibers were cross-linked with glutaraldehyde to improve their stability and mechanical performance (Chase and Kushmerick, 1988). End fixation was achieved by mounting the fibers by means of their T-clips on two stainless steel hooks so that the fibers were suspended in a bath containing fresh rigor solution (see Table 1). A Pasteur pipette that had been heat-pulled to a fine tip and mounted on an X-Y manipulator was used to deliver by gravity-feed a fine stream of solution consisting of rigor solution with, in addition, 30% glycerol and 0.5% glutaraldehyde. The stream of solution could be seen clearly through the glass walls of the bath by means of a dissecting microscope. The stream of fixing solution was positioned to come in contact with each T-clip and the first 0.1–0.5 mm of fiber at each fiber end for 2–3 s. The fixed region of the fiber could be identified under the dissecting microscope by the difference in the refractive index of the fixed compared with the unfixed region and by the slight shrinkage of the fiber. The T-clips were tightened around the fiber, and the fiber was mounted on the apparatus. Under the compound microscope, there appeared to be a sharp boundary between the fixed and unfixed regions of the fiber. The sarcomere length of the muscle fibers was adjusted to 2.4 μm, and the fiber width and depth were measured microscopically (Zeiss 40x, NA 0.75 water immersion objective, Leitz 25x Periplan eyepiece) to calculate the cross sectional area (Blinks, 1965).

The apparatus

The apparatus was a modification of that described previously (Ferenczi, 1986). Troughs cut in a temperature-controlled stainless steel block were used to hold the muscle fiber. The first trough had a quartz side to allow illumination of the caged ATP solution by the photolysis light. The width of this trough was 0.8 mm, and its volume was 25 μl. One end of the muscle fiber was attached to a stainless steel hook glued to a silicon strain gauge (AE 801, AME, Horten, Norway). A layer of oil of adjustable thickness between the back of the silicon strain gauge and a movable brass plate was used to critically damp the transducer oscillations. The other end of the

TABLE 1 Constitution of experimental solutions

Solution name	TES	MgATP	EGTA	EDTA	Creatine Phosphate	Propionate	Glutathione	Caged ATP	Free Ca^{2+}	Free Mg^{2+}
Mg-Rigor	60	0	30	0	14.1	0	0	0	0	2
EDTA-Rigor	60	0	30	2	0	38	0	0	0	0
EDTA-Rigor with CP	60	0	30	2	12.5	0	0	0	0	0
Relaxing	60	5	30	0	3.8	0	1	0	0	2
Pre-activating	60	5	0	0	33.9	0	1	0	0	2
Activating	60	5	30	0	4.3	0	1	0	0.032	2
Caged ATP	60	0	30	0	11.7	0	10	5 or 10	0	2

pH 7.1; ionic strength = 0.15 M, 20°C (concentrations are given in mM).

The ionic strength was calculated using a modified version of the computer program used in Ferenczi et al. (1984) by varying the concentration of potassium propionate or creatine phosphate. In the case of solutions of caged ATP, the contribution of caged ATP to the ionic strength was assumed to be equal to that contributed by an equal concentration of ADP. 10 mM glutathione was present in all photolysis solutions to reduce fiber damage caused by the photolysis by-products. In activating solution, to obtain a free Ca^{2+} concentration of 0.032 mM, 30 mM total Ca^{2+} was added.

Abbreviations: TES, 2-(N-tris[hydroxymethyl]methylamino)ethanesulfonic acid; EDTA, Ethylenediaminetetraacetic acid; EGTA, Ethylene glycol bis-(β-aminoethyl ether)N,N,N',N' tetraacetic acid; CP, creatine phosphate.

muscle fiber was connected to a motor (Model 300S, Cambridge Instruments, Cambridge, MA) that allowed rapid adjustments to the muscle length. 50 ns light pulses from a ruby laser (Laser Applications, Inc., Winter Park, FL) were frequency-doubled by means of a temperature-stabilized, angle-tuned potassium dihydrogen phosphate crystal to produce light pulses with an energy of up to 300 mJ at 347 nm. The light intensity was adjusted to the desired value by rotating a stacked-plate polarizer in the beam. The laser beam cross section was compressed to an ellipse (8 × 3 mm for the long and short axes, respectively) to illuminate all the area of the experimental trough quartz window.

Protocol

A muscle fiber was mounted in the apparatus in relaxing solution and transferred to a trough containing pre-activating solution for 2 min (Moisescu, 1976), and then to a trough containing activating solution. Once the isometric plateau was reached (~200 kN m^{-2}), the fiber was returned to relaxing solution. The width and thickness of the fiber were measured, and then the fiber was transferred to rigor solution: initially, EGTA-rigor solution to optimize the rate of substrate removal by chelation of Mg^{2+}, then Mg-rigor solution. Tension rose rapidly to a rigor tension level of 20–70 kN m^{-2}. After 2 min, the fiber was transferred to caged ATP solution (either NPE-caged ATP or DMB-caged ATP). After 2 min incubation, the fiber tension was adjusted to the desired level by stretching or releasing the fiber, and the laser was fired to cause the photorelease of ATP and the relaxation of the fiber tension. After relaxation, the fiber was transferred to relaxing solution and the experimental protocol was repeated. In most experiments, the Mg-rigor solution and the caged ATP solution contained 10.5 units ml^{-1} of apyrase to remove contaminating ADP. The apyrase treatment markedly reduced the tendency of caged ATP to induce a decay in rigor tension before photolysis: a phenomenon that otherwise occurs readily (Goldman et al., 1984a).

Data collection and analysis

The tension data were collected using a digital oscilloscope (Tektronix 5223) and transferred to a personal computer for display, storage, and analysis. After apyrase treatment, tension records after photolytic release of ATP generally decayed monotonically and could be treated as single exponential processes. We also used the algebraic difference approach introduced by Goldman et al. (1984a) to provide a treatment of tension records that had complex time courses. This was done by releasing ATP from caged ATP in paired experiments that differed in the initial rigor tension. Records were then subtracted to obtain a difference trace. The tensions had a tendency to converge, i.e., the difference tended toward zero, after 100 ms. Difference traces that could be treated as single exponential processes could then be used to calculate the rate of ATP-induced cross-bridge detachment after taking into account the kinetics of caged ATP photolysis (see below).

The statistical tests were obtained from Harnett (1975), and means are given plus or minus 1 SEM with the number of experiments in brackets.

Computational methods

The model was calculated using a Euler-stepping routine for the set of differential equations describing the incremental change in the concentration of each constituent. The program written in FORTRAN ran sufficiently fast on a personal computer (33 MHz Intel 486) not to require more sophisticated algorithms. The model calculated with time intervals of 0.1 or 1 μs gave superimposable results.

RESULTS

^{31}P NMR spectra of caged ATP compounds

In spectra measured at pH 9.5, NPE-caged ATP has been reported to show signals for the α-, β-, and γ-phosphates,

respectively, at δ −8.3 (doublet), −20.3 (triplet), and −9.4 p.p.m. (doublet), with no splitting of the γ-phosphorus signal caused by the presence of two diastereoisomers, although in S-caged ATP(γS), which also has two diastereoisomers, the γ-phosphate signal was split into two doublets differing in chemical shift by 0.17 p.p.m. (Walker et al., 1988). Under our experimental conditions (pH 7.0), the ^{31}P NMR spectrum of NPE-caged ATP showed two well resolved doublets for the γ-phosphate at δ −11.66 and −11.72 p.p.m. The α- and β-phosphate signals appeared at δ −10.75 and −22.48, respectively. Reexamination of the original ^{31}P NMR spectrum of NPE-caged ATP (Walker et al., 1988), kindly made available by Dr J. W. Walker, showed that the γ-phosphorus signal was indeed present as two poorly resolved doublets, but this was obscured by the high noise level of that spectrum. The mean 2.3 p.p.m. difference in chemical shift between corresponding nuclei in our spectrum of NPE-caged ATP and that of Walker et al. (1988) probably arises from the use of different H$_3$PO$_4$ reference standards.

In DMB-caged ATP, the presence of two diastereoisomers caused more profound effects, because all three phosphorus nuclei showed separation into distinct signals. Thus, the α-phosphate appeared as two doublets at δ −10.52 ($J_{\alpha\beta}$ 19.5 Hz) and −10.60 p.p.m. ($J_{\alpha\beta}$ 18.3 Hz), and the γ-phosphate also gave two doublets at δ −11.65 ($J_{\beta\gamma}$ 15.8 Hz) and −11.73 p.p.m. ($J_{\beta\gamma}$ 15.9 Hz). The β-phosphate signal contained eight lines, i.e., two overlapping doublets of doublets, centered at δ −21.86 and −21.95 p.p.m. We have not attempted to assign the two sets of resonances to individual diastereoisomers.

Spontaneous DMB-caged ATP hydrolysis

HPLC analysis of samples of DMB-caged ATP incubated at varying pH values (see Materials and Methods) showed that ADP and 3′,5′-dimethoxybenzoin phosphate were predominant products that formed in parallel. We have described elsewhere a likely mechanism for the specific hydrolysis of DMB-caged ATP (Corrie and Trentham, 1993), which involves participation of the carbonyl group in the benzoin cage. The breakdown of the compound accelerated as the pH was raised. DMB-caged ATP hydrolyzed at 0.023 h^{-1} at pH 9.5 and at 0.00024 h^{-1} at pH 7.0. Thus, a 10 mM solution of DMB-caged ATP generates 2.4 μM ADP h^{-1} at 30°C and pH 7.0. NPE-caged ATP was stable under all conditions investigated here. The main photochemical characteristics of NPE- and DMB-caged ATP are summarized in Table 2.

Effect of apyrase treatment on isometric tension and the relaxation time course

Before testing the effect of apyrase treatment on the kinetics of relaxation from rigor in muscle fibers, we determined the effect of apyrase treatment on isometric tension. Addition of apyrase had no effect on the isometric tension: in six fibers, tension values were 207 ± 18 kN m^{-2} and 211 ± 20 kN m^{-2} in the presence and absence of apyrase, respectively.

TABLE 2   Comparative photochemical properties of caged ATP reagents

Parameter	NPE-caged ATP	DMB-caged ATP
Quantum yield	0.63*	0.3[‡]
Extinction coefficient at 347 nm (M^{-1} cm^{-1})	660*	170[‡]
Release rate of ATP on photolysis (s^{-1})	118[¶]	>10^5 [‡§]

* Walker et al. (1988).
[‡] Corrie and Trentham (1993).
[§] Corrie et al. (1992).
[¶] Goldman et al. (1984a).

Apyrase had a marked accelerating effect on the time course of relaxation from rigor (Fig. 2). This effect is attributed to the removal of low levels of ADP from the experimental trough solution and the muscle fiber before flash photolysis of DMB-caged ATP. Treatment of the rigor fiber and of the caged ATP relaxing solution with apyrase leads to the suppression of the characteristic "hump" or transient rise in tension in the relaxation profile observed previously (Goldman et al., 1984a).

This interpretation of the result shown in Fig. 2 was tested by additions of low concentrations of ADP to experimental solutions containing NPE-caged ATP after treatment of the solution with immobilized apyrase (Fig. 3 *a*). A simple kinetic scheme based on the model of Goldman et al. (1984b), but which incorporates ADP binding to A.M cross-bridges described below (Fig. 3 *b*), is shown to reproduce the main features of the data in Fig. 3 *a*. A shoulder in the relaxation

profile appears at ADP concentrations of 5 μM and above, and this shoulder becomes a hump at an ADP concentration of 50 μM.

The effect of apyrase treatment was greater for solutions containing DMB-caged ATP than for solutions containing NPE-caged ATP, as expected from the slow spontaneous decomposition of DMB-caged ATP to ADP and DMB-caged P$_i$. Relaxations were generally faster when the rigor muscle fiber as well as caged ATP solutions were treated with apyrase compared with situations where only the caged ATP solution was treated with immobilized apyrase and the apyrase was subsequently removed. This suggests that a low level of ADP remains in rigor muscle fibers, presumably because of some myofibrillar sites with high affinity for ADP.

Although relaxation time courses were largely monophasic, a slow, low amplitude component was often present. We examined this using the approach of Goldman et al. (1984a) by taking the algebraic difference of tension records. The half-times for relaxations were approximately the same whether calculated from the raw data or from difference traces. This was observed both for DMB-caged ATP and NPE-caged ATP. The relaxation traces of high and low initial tension converged late in the relaxation time course when the tension was at or near zero (convergence was observed for tension levels of 2.53 ± 0.53 kN m^{-2} ($n = 19$), or about 5% of the initial rigor force for the 6 fibers used). The rate of relaxation measured from the difference of these traces was the same as the mean rate of relaxation of the high and low initial tension traces. This indicates that in the presence of apyrase there is essentially no re-attachment of cross-bridges and that the rate of cross-bridge detachment is being observed directly.
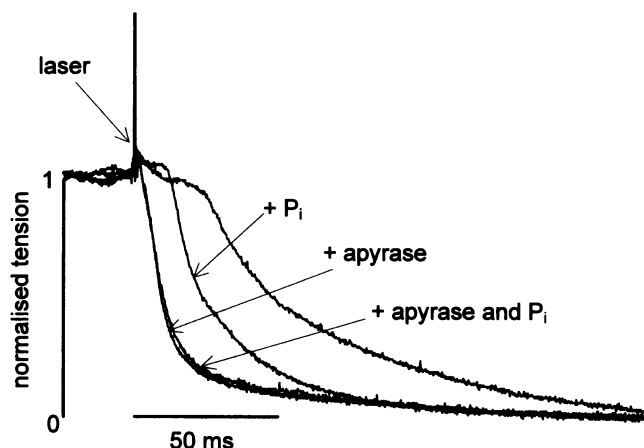

FIGURE 2   The effect of addition of apyrase and P$_i$ on the relaxation time course. Relaxation time courses were obtained by laser flash photolysis of 10 mM DMB-caged ATP at 20°C with the muscle fiber held at a sarcomere length of 2.35 μm. Each flash caused the photorelease of 0.66 to 0.90 mM ATP. The first flash was carried out before treating the fiber with apyrase, and in the absence of added P$_i$. The second flash was carried out in the presence of 8 mM P$_i$. A marked acceleration of relaxation is obtained, but a lag in the relaxation is still seen. Relaxation induced by photolysis of DMB-caged ATP after treatment with apyrase, and in the absence of P$_i$ (flash 3) does not show the lag seen in the two previous relaxations. Increasing P$_i$ to 8 mM (flash 4) now has no accelerating effect on the relaxation time course. These records have been normalized for the pre-flash tension. Before normalization, rigor tension values were similar: 42, 35, 29, and 38 kN m^{-2} for flashes 1 to 4, respectively.

Dependence of the relaxation time course on P$_i$

In an active muscle fiber, P$_i$ is thought to promote the reversal of some steps in the cross-bridge cycle, resulting in actomyosin dissociation and a reduction in isometric tension (Hibberd et al., 1985; Cooke and Pate, 1985). In terms of Scheme 1 these steps are:

$$A.M.ADP + P_i \leftrightarrow A.M.ADP.P_i \leftrightarrow M.ADP.P_i$$

Addition of 8 mM P$_i$ to DMB-caged ATP solutions treated with apyrase (Fig. 2) did not affect the time course of relaxation, indicating that relaxation observed involves only ATP binding and actomyosin dissociation steps in Scheme 1 and does not involve cross-bridges that have undergone re-attachment to the thin filament. However, without apyrase treatment, P$_i$ did affect the relaxation kinetics as observed previously (Hibberd et al., 1985).

The effect of adding 8 mM P$_i$ on the time course of relaxation in the presence of apyrase was further investigated using NPE-caged ATP at 20°C in paired trials. Relaxation records were obtained from the same fiber with similar concentrations of ATP released upon photolysis. After apyrase treatment, the mean rate of relaxation was 61.2 ± 6.4 s^{-1} ($n = 14$) in the presence of 8 mM P$_i$ and 59.4 ± 6.9 s^{-1} ($n = 10$) in the absence of added P$_i$. Assuming a normal
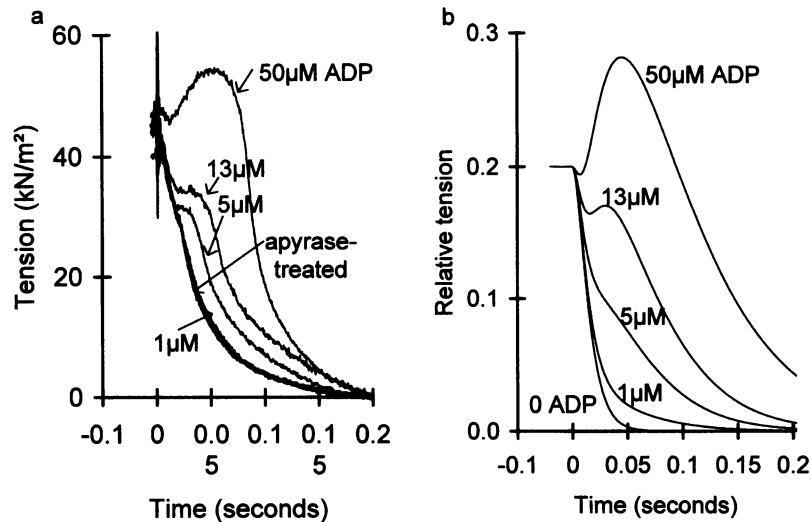
FIGURE 3   (a) Effect of ADP on the relaxation time course from rigor in a permeabilized fiber at 20°C, sarcomere length: 2.6 μm. The NPE-caged ATP solution was treated with immobilized apyrase and the time course of relaxation from rigor measured as explained in the text. The experiment was repeated on the same fiber after addition of known concentrations of ADP as shown. Relaxation was initiated at zero time by laser-flash photolysis of 5 mM NPE-caged ATP releasing ~1 mM ATP. Initial rigor tension levels were adjusted to be similar in each experiment. The "apyrase-treated" and "1 μM ADP" traces can be differentiated by the slight shoulder in the relaxation profile of the latter. (b) Simulation of the data using the model described in Schemes 2 and 3 for photolysis of NPE-caged ATP releasing 1 mM ATP, and in the presence of 0, 1, 5, 13, and 50 μM ADP. The values for the rate constants used in the simulation are as given in the text, namely $k_1 = 1 \times 10^5$ M^{-1} s^{-1}, $k_2 = 100$ s^{-1}, $k_3 = 35$ s^{-1}, $k_4 = 1 \times 10^6$ M^{-1} s^{-1}, and the appearance of 1 mM ATP by photolysis occurs with a rate constant $k_c = 118$ s^{-1}. The concentration of cross-bridge pairs is 0.1 mM.

distribution of these data, the two-tailed 95% confidence limits on the difference in the rate of relaxation with or without 8 mM P_i is 1.9 ± 5.9 s^{-1} (mean difference ± 95% confidence limit; $n = 10$, data are taken from 9 fibers), suggesting that P_i does not affect the relaxation kinetics.

## Dependence on initial rigor tension

The effect of initial rigor tension on the time course of relaxation from rigor is shown in Fig. 4. With DMB-caged ATP, a dependence of the relaxation rate on the initial rigor tension was observed and is described by a linear relationship of slope 0.75 ± 0.12 m^2 s^{-1}kN^{-1} and intercept 32.3 ± 7.1 s^{-1} (Fig. 4). A similar relationship was observed in an ex-

periment using NPE-caged ATP (data not shown). F-tests indicate that a linear relationship helps to explain the stress dependence ($t_{(46df)} = 8.0$, $p < 0.0005$ and $t_{(43df)} = 5.5$, $p < 0.001$ for DMB-caged ATP and NPE-caged ATP, respectively). The data indicate that ATP binding or cross-bridge dissociation rates are strain-sensitive as previously inferred from the difference of tension records (Goldman et al., 1984a).

Dependence of relaxation on the concentration of ATP produced by photolysis of caged ATP

The ability of the two caged ATP compounds to relax muscle fibers was compared using 16 apyrase-treated fibers and so-

FIGURE 4   The effect of cross-bridge strain on the relaxation time course. The initial rigor tension was varied for 11 fibers ($n = 53$), and the half-time for relaxation was measured. Experiments were carried out with apyrase-treated solutions, using 10 mM DMB-caged ATP. The released ATP concentration varied between 0.49 and 1.02 mM. The continuous line represents a linear regression to the data with a slope of 0.75 ± 0.12 m^2 s^{-1} kN^{-1}.
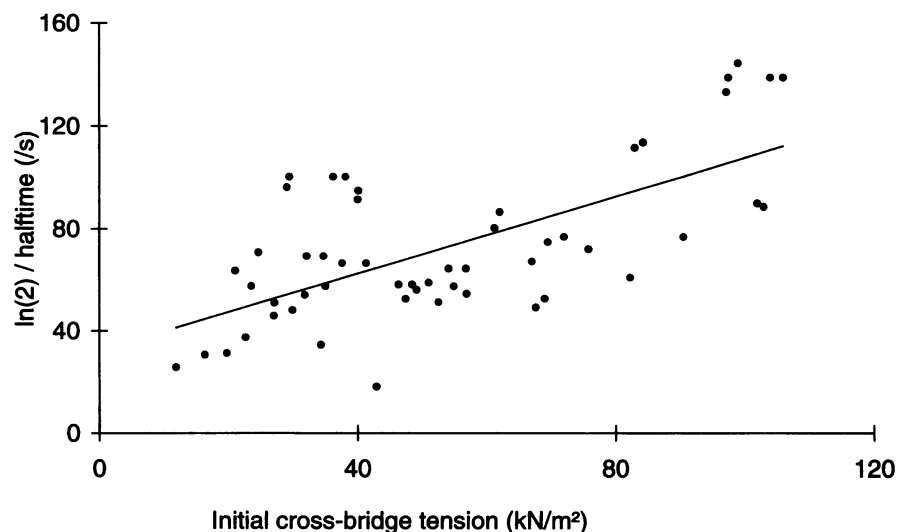
lutions, and 5 mM NPE-caged ATP or 10 mM DMB-caged ATP to release ATP. The highest concentration of ATP that was released from DMB-caged ATP was 1.1 mM compared with 2.8 mM ATP from NPE-caged ATP. The rate of relaxation was dependent on the concentration of photogenerated ATP as shown in Fig. 5. For an ATP concentration range of 0.42–0.79 mM using DMB-caged ATP, the mean relaxation rate was 58.6 ± 9.7 s^{-1} ($n = 9$), and for NPE-caged ATP, the corresponding mean rate was 42.1 ± 4.4 s^{-1} ($n = 9$). The difference in relaxation rate was not significant for this concentration range ($t_{(16df)} = 1.57$, $p > 0.1$). For an ATP concentration range of 0.8–1.1 mM using DMB-caged ATP, the mean rate of relaxation was 101.7 ± 10.6 s^{-1} ($n = 9$), and for NPE-caged ATP the mean rate of relaxation was 38.3 ± 6.2 s^{-1} ($n = 7$). The difference in relaxation rate for this ATP concentration range was significant ($t_{(13df)} = 5.96$, $p < 0.001$). Thus, it is only over a fairly narrow concentration range of released ATP that DMB-caged ATP photolysis induces a significantly faster relaxation.

DISCUSSION

Synthesis and properties of DMB-caged ATP

The new caged ATP reagent was synthesized by coupling DMB-caged P$_i$ with ADP, using N,N'-carbonyldiimidazole to activate the caged P$_i$ (Hoard and Ott, 1965). The slow spontaneous hydrolytic reversion of DMB-caged ATP to DMB-caged P$_i$ and ADP necessitated particular care during its purification to avoid prolonged exposure to alkaline pH or elevated temperatures. Despite these precautions, freshly prepared DMB-caged ATP was always contaminated with a small amount, typically 1%, of ADP. As described elsewhere

(Corrie and Trentham, 1993), the hydrolysis is a specific consequence of the nature of the DMB-protecting group. The same hydrolysis mechanism is not available to NPE-caged ATP, which therefore does not spontaneously generate ADP. Photolysis of DMB-caged ATP is less efficient than that of NPE-caged ATP because, as shown in Table 2, both the quantum yield and the extinction coefficient at 347 nm are lower. The combination of these factors has meant that in the experiments described here, the maximum available ATP release from DMB-caged ATP was limited to 1 mM.

The low quantum yield is of some interest because we have previously reported that for DMB-caged P$_i$ the quantum yield is 0.78 (Corrie and Trentham, 1992). These data suggest that for DMB-caged ATP there may be an additional nonphotolytic pathway from the excited state, presumably via an interaction with the purine. By altering the substituents on the benzoin, it may be possible to avoid this pathway and regain a high quantum yield.

The origin of the "hump"

Goldman et al. (1984a) considered that the hump was a manifestation of cooperative phenomena leading to thin filament activation (Bremel and Weber, 1972; Bremel et al., 1973), where the presence of attached cross-bridges maintains the activated state of neighboring myosin binding sites on the thin filament. Consequently, cross-bridges detaching rapidly may rebind to actin and go through a force-generating cycle, even in the absence of calcium ions, resulting in a transient tension rise. It is only when a sufficient number of cross-bridges have detached that thin filament activation disappears, allowing complete relaxation of the muscle fiber. The
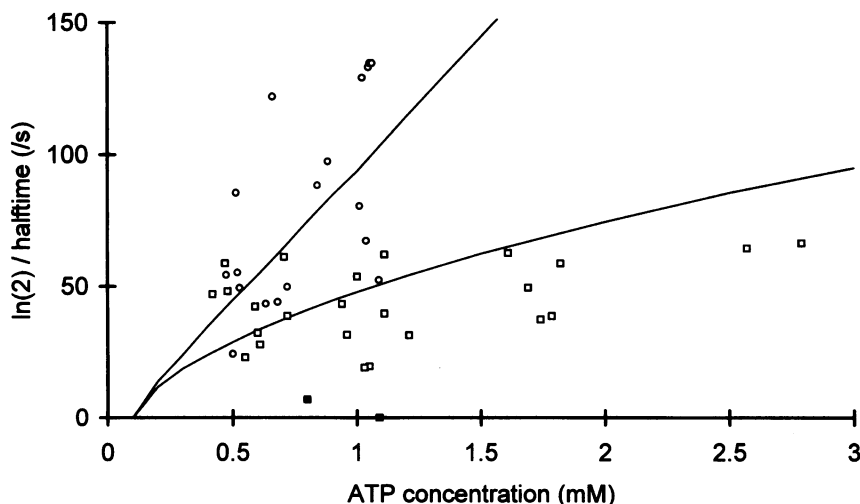

FIGURE 5 The relationship between the relaxation time course and the ATP concentration released by photolysis. Data obtained by photolysis of DMB-caged ATP (○), photolysis of NPE-caged ATP (□), photolysis of NPE-caged ATP (■)—but these 2 data points were not included in the statistical analysis because they fall outside 2 SEM. These data have been corrected for the effect of initial cross-bridge tension using the separate values of tension dependence of NPE- and DMB-caged ATP described in the text and Fig. 4. The continuous lines were obtained by simulation of the model shown in Scheme 3, with a second order rate constant for ATP binding (k_1) of 1×10^5 M^{-1} s^{-1} and other rate constants defined in the text, in the absence of ADP. The lower line was obtained with a rate constant for photolysis (k_c) of 118 s^{-1} simulating photolysis of NPE-caged ATP, whereas the upper line was obtained with $k_c = 1 \times 10^5$ s^{-1}, simulating photolysis of DMB-caged ATP. In the absence of added ADP, simulation of the model shown in Scheme 3 results in relaxation kinetics identical to those produced by the model of Goldman et al. (1984a).

experiments shown here suggest that ADP has a predominant role in determining the shape of the relaxation time course. We suggest that it is the presence of A.M.ADP cross-bridges that is responsible for the maintenance of thin filament activation, and that A.M cross-bridges do not promote the cooperative behavior on thin filaments. In the absence of ADP, the time course of relaxation is fast and monotonic. Addition of ADP to the rigor muscle fiber generates A.M.ADP cross-bridges and slows down relaxation. Even in the presence of added ADP, there is a small and rapid initial phase of tension relaxation that precedes the shoulder or hump in the relaxation profile. This indicates that A.M.ADP cross-bridges have a slower rate of detachment than A.M cross-bridges and prevent thin filament deactivation long enough to allow reattachment of the rapidly detaching A.M cross-bridges. Such an interpretation was modeled as shown in Figs. 3 *b* and 6.

Three experimental observations support the idea that ADP is responsible for slow relaxation and the hump. First, the addition of known concentrations of ADP to caged ATP solutions that had been previously treated with immobilized apyrase caused the size of the hump to increase as the ADP concentration increased (Fig. 3 *a*). Second, the addition of 8 mM inorganic phosphate to the apyrase-treated DMB-caged ATP solution did not accelerate the rate of relaxation (Fig. 2). Third, in the presence of apyrase the rate of convergence of high and low initial tension relaxation records was the same as the mean rate of relaxation of corresponding records.

Studies in cardiac and smooth muscle have also shown the important role of ADP in modifying relaxation kinetics and that P_i does not accelerate relaxation in the absence of ADP (Fuglsang et al., 1993; Martin and Barsotti, 1991, 1994; Nishiye et al., 1993). In the case of cardiac muscle, the influence of ADP closely parallels what we observe with skeletal muscle. In smooth muscle, the effects appear to be longer lasting in that the time for relaxation is very much prolonged by the presence of ADP, especially in tonic smooth muscle and it appears impossible to remove final traces of ADP with apyrase. These different properties may be linked to the capacity of smooth muscle to exhibit the "latch" state (Fuglsang et al., 1993).

In all three muscle types, the absence of a P_i effect on the fast phase of relaxation is striking and provides evidence that P_i effects are solely related to product release steps during fiber ATPase activity as previously proposed (Hibberd et al., 1985; Cooke and Pate, 1985).

Effects of the rate of ATP release and of ATP concentration on tension relaxation

Our data suggest that the rate of release of ATP from NPE-caged ATP partially limits the rate of relaxation of rigor tension. For ATP concentrations 0.8–1.1 mM, the mean rate of relaxation initiated by NPE-caged ATP was 38.3 ± 6.2 s^{-1} ($n = 7$), whereas the mean rate of relaxation with DMB-caged ATP was 101.7 ± 10.6 s^{-1} ($n = 9$). The computer simulation of relaxation transients also indicates this relationship between the rate of ATP release and the rate of

relaxation (Fig. 5). In a further simulation (not shown), increasing the photolysis rate of ATP release above 10^5 s^{-1} for DMB-caged ATP did not further increase the rate of relaxation.

On photolysis of DMB-caged ATP, no plateau was reached in the rate of relaxation as the concentration of ATP released increased (Fig. 5). In the case of photolysis of NPE-caged ATP, a leveling in the rate was observed at high ATP concentrations, but the rate was less than that induced by photolysis of DMB-caged ATP, presumably because of other factors, such as the slower rate of photolysis. Thus, we were not able to observe the cross-bridge detachment step directly; the process was always limited at least in part by the ATP-induced process.

The second order association rate of ATP to A.M that gave the best fit to the experimental data was 1×10^5 M^{-1} s^{-1}, which is 10-fold lower than the value found for the dissociation of myofibrils at 4°C (e.g., Houadjeto et al., 1992) and also fivefold lower than that derived previously in fibers with NPE-caged ATP photolysis by Goldman et al. (1984a) using the algebraic difference approach (see data collection and analysis). Thus, our more direct estimate of the ATP-induced relaxation rate is even more different from the myofibrillar kinetics than that estimated by the algebraic difference method. The series compliance of muscle fibers may reduce the observed relaxation rates (Luo et al., 1993) so that variability in the fiber attachments that may result in variations in fiber compliance could account for inter-fiber differences in the relaxation rates and for differences between our results and that of others. Other possible reasons are effects caused by caged-ATP binding to cross-bridges and that the observed rates relate to different populations of cross-bridges; we consider both of these possibilities below.

Caged ATP binding to muscle fibers

Experiments (H. Higuchi and Y.E. Goldman, personal communication; Thirlwell et al., 1994) carried out in the presence of Ca^{2+} have shown that at low MgATP concentrations ($\sim$100 μM) the presence of millimolar concentrations of NPE-caged ATP or DMB-caged ATP causes significant reduction in the maximal shortening velocity of muscle fibers, indicative of competitive inhibition of ATP binding by caged ATP under unloaded conditions. The data of Thirlwell et al. (1994) suggest a K_i of 1–2 mM. The experiments described here were performed under isometric conditions in the presence of 10 mM caged ATP (but in the absence of Ca^{2+}, which may influence nucleotide binding (Rosenfeld and Taylor, 1987a, b)). There may be quantitative effects of competitive inhibition by caged ATP as manifested in the tendency of the relaxation kinetics to saturate on the release of high concentrations of ATP from NPE-caged ATP (Fig. 5), but it is unlikely that competitive inhibition would affect qualitatively our interpretation of the role of ADP in relaxation. It has been suggested that one diastereoisomer of NPE-caged ATP ("isomer A") binds to cross-bridges in rigor in the absence of Ca^{2+} with higher affinity than the other diastereoi-

somer (Dantzig et al., 1989). We consider that much of the observed difference may have been caused by ADP contamination in isomer A.

Comparison of relaxation kinetics with other biophysical measurements

The maximum relaxation rate of 130 s^{-1}, initiated by DMB-caged ATP, is slower than the rate of 200 s^{-1}, initiated by NPE-caged ATP, at 10–12°C for the change in the (1,0) and (1,1) equatorial x-ray diffraction intensities accompanying muscle relaxation (Poole et al., 1991). The diffraction signal is also considered to show the rate of cross-bridge detachment. The reason for the difference may be that the x-ray signal reflects the behavior of a population of cross-bridges other than those detected by the tension signal. On the other hand, the maximal relaxation rate observed here is comparable with the fast phase of the stiffness (43 s^{-1}) and birefringence signals (63 s^{-1}) induced by photolysis of NPE-caged ATP observed at 15°C (Peckham et al., 1994).

## A model of the effect of ADP on relaxation kinetics

A model was developed to account for the effect of ADP on the relaxation time course, based on the model of Goldman et al. (1984b) with incorporation of ADP binding to A.M cross-bridges as shown in Scheme 2.
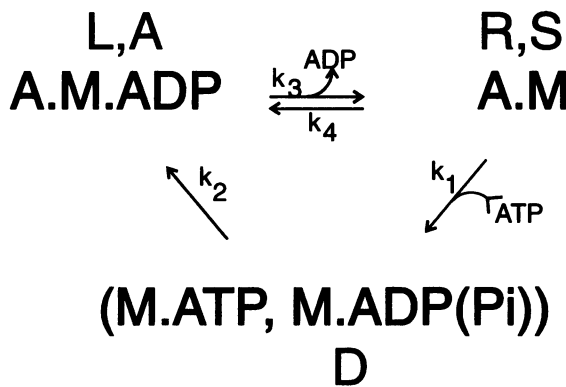
Scheme 2

The model considers pairs of cross-bridges. Each member of a pair can be in one of three states: two attached states and one detached state. Initially, all cross-bridges are attached to the thin filaments, either in A.M.ADP (L) or A.M states (R). The distribution of cross-bridge pairs (zero, one, or two ADP bound to each pair) depends on the ADP concentration and the affinity of A.M cross-bridges for ADP. The tension developed by the initial rigor cross-bridges depends on the arbitrary extension of the fiber and, in Fig. 3 b, is given a value of 0.2 of the actively generated force. After ATP binding, A.M cross-bridges detach (D). Cross-bridge re-attachment is possible, even in the absence of calcium, if the other cross-

bridge of a pair is one of the original rigor cross-bridges in the A.M.ADP state (L). In this case, the re-attached cross-bridge (A) generates active tension, given a normalized value of 1. Upon losing ADP, the re-attached cross-bridge (now S) generates the same tension as A and is therefore distinct from R. Cross-bridge S then detaches in the normal way. Re-attachment is only possible for a detached cross-bridge (D) that exists in a pair of cross-bridges in the LD state. All intermediates and pathways of the model are shown in Scheme 3, with re-attachment shown in bold:
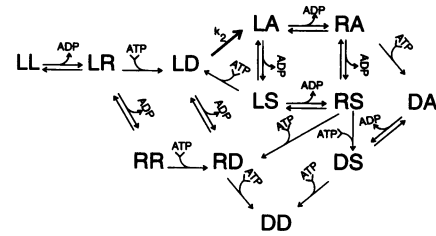
Scheme 3

where $k_1 = 1 \times 10^5$ M^{-1} s^{-1}, $k_2 = 100$ s^{-1}, $k_3 = 35$ s^{-1}, $k_4 = 1 \times 10^6$ M^{-1} s^{-1} (see Scheme 2), and where photolysis of caged ATP produces 1 mM ATP, with a rate $k_c = 118$ s^{-1} or 1×10^5 s^{-1} for NPE- or DMB-caged ATP, respectively (Figs. 3 b and 6 a). The choice of rate constants is a compromise between fitting the experimental data and using reasonable values to describe the reaction pathway (see also Dantzig et al., 1991; Goldman et al., 1984b).

Defining K as k_4/k_3, and XX as the total concentration of cross-bridge pairs in the fiber (0.1 mM in the model), then before photolysis, the concentration of cross-bridge states LR, RR, and LL depends on ADP concentration as follows:

$$LR = 2 \times K \times ADP \times XX/(K \times ADP + 1)^2$$

$$RR = XX/(K \times ADP + 1)^2$$

$$LL = K^2 \times ADP^2 \times XX/(K \times ADP + 1)^2$$

After the photolysis light pulse, the rate of change of each reactant is given by 1 of 15 differential equations of the type shown below.

$$dLR/dt = 2 \times LL \times k_3 + 2 \times RR \times k_4 \times ADP$$
$$- LR \times (k_4 \times ADP + k_1 \times ATP + k_3)$$
$$dLA/dt = LD \times k_2 + (RA + LS) \times k_4 \times ADP$$
$$- 2 \times LA \times k_3$$
$$dDD/dt = (DS + RD)k_1 \times ATP$$

etc.

In Figs. 3 b and 6 a, we consider that the fiber is bathed in a relatively large volume, so that the concentration of ADP remains constant and $dATP/dt = cATP \times k_c$, where $cATP$ is the concentration of caged ATP that photolyzes. We have also tested the situation where diffusion of
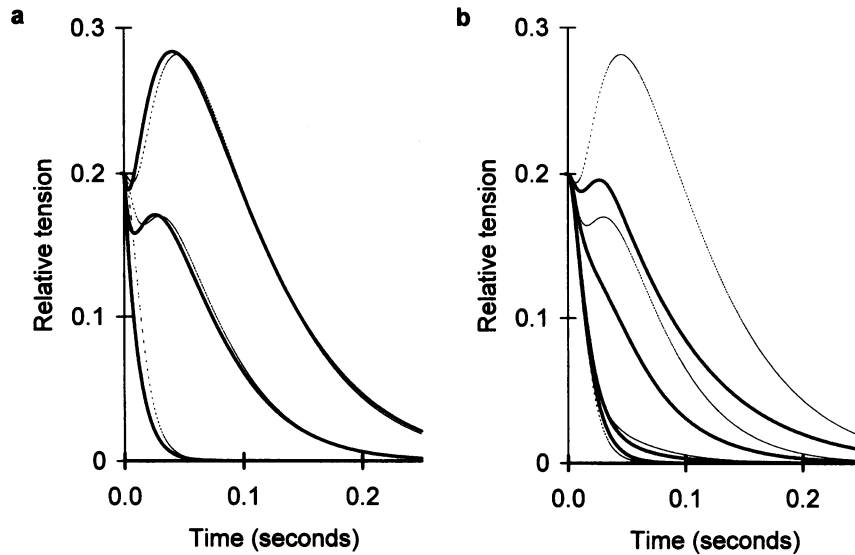
FIGURE 6   (a) Comparison of the relaxation time-courses predicted by the model in Schemes 2 and 3 for the photolytic release of 1 mM ATP from DMB-caged ATP (*solid line*) and NPE-caged ATP (*thin dashed line*), where the photolysis rate constants are 1×10^5 s^{-1} and 118 s^{-1}, respectively, with the same values for the other rate constants as for Fig. 3 b. Time-courses for 0, 13, and 50 μM ADP are shown. (b) Comparison of the relaxation time course predicted by the model if it is considered that diffusion is slow on the time scale of the experiment (*solid line*). In this case, the free concentrations of ATP and ADP are affected by binding to the muscle cross-bridges. The thin dashed line is that for the model of Figs. 3 b and 6 a for the situation where diffusion is fast, i.e., that the concentration of ATP is determined solely by the extent and kinetics of caged ATP photolysis and the concentration of ADP is constant. The figure shows calculations for NPE-caged ATP releasing 1 mM ATP and in the presence of 0, 1, 13, and 50 μM ADP, and the same values for the rate constants as for Fig. 3 b.

nucleotide in and out of the fiber is slow compared with the time course of the relaxation (Fig. 6 b). In this case, the experimental volume is limited to the fiber volume and the concentration of ATP and ADP is significantly affected by binding to the cross-bridges. then,

$$\frac{dATP}{dt} = cATP \times k_c - k_1 \times ATP$$

$$\times (LR + 2 \times RR + LS + RA + 2 \times RS + DS + RD)$$

and

$$ADP = ADP_{total} - 2 \times LL - LR - LD$$

$$- 2 \times LA - LS - RA - DA.$$

Note that in this case at time 0, the concentrations of *LL*, *LR*, and *RR* depend on the concentration of ADP, and the concentrations of LD, LA, LS, RA, and DA are zero. In each case, the force developed by the fiber is given by

RELATIVE FORCE

$$= (F \times (2 \times LL + 2 \times RR + 2 \times LR$$

$$+ LD + RD + RA + LA + RS + LS)$$

$$+ (LA + LS + RS + RA + DA + DS))$$

$$\div 2 \times XX,$$

where *F* is the fractional force attributed to the initial rigor cross-bridges, in this instance, $F = 0.2$, whereas the force produced after re-attachment (A and S) is 1.

The model accounts for the most prominent features of the relaxation time-courses seen in Figs. 2 and 3 a, where the effect of ADP is accommodated by simple cooperative behavior for cross-bridge re-attachment. The ADP dissociation constant of 35 μM used in the model (k_3/k_4) is comparable with the measured value ($K_d = 18$ μM, Dantzig et al., 1991). The discrepancy between the experiment in Fig. 3 a and the model of Fig. 3 b at low concentrations of ADP may be accounted for by some residual ADP contamination (1–2 μM) in the experiment. The records shown in Fig. 2 in the presence of apyrase show a faster relaxation than in Fig. 3 a and more closely match the simulation at zero ADP in Fig. 3 b. In some fibers, there may be residual ADP despite apyrase treatment. In smooth muscle strips, it also appeared difficult to remove the last traces of ADP with apyrase (Nishiye et al., 1993).

The decay of tension after the hump is steeper than the model predicts. This phenomenon was studied by Dantzig et al. (1991), who noted that, although striation spacings remained constant over about 50 ms, the spacing abruptly changed just before the steep tension decline. From these and other analyses, Dantzig et al. (1991) concluded that above a certain tension threshold per attached cross-bridge, rapid relaxation was initiated. This nonlinear response is not included in the model, which may account for the discrepancy between the shape of the observed and predicted relaxations in the presence of 50 μM ADP.

When diffusion of nucleotide in and out of the fiber is treated as being slow compared with steps of the cross-bridge cycle, the time course of relaxation is modified as shown in

Fig. 6 *b*. The main features of the relaxation profile remain, i.e., a monotonic decay at low ADP concentrations but a transient tension rise at higher ADP concentrations. The effect of ADP is less marked in the slow diffusion model, but altering rate constants restores sensitivity. For example, reducing k_3 from 35 to 20 s^{-1} (and, coincidentally, bringing the ADP dissociation constant closer to its measured value, Dantzig et al., 1991) restores the ADP sensitivity shown by the fast diffusion model (simulation not shown). Investigation of the properties of the models suggests that the behavior of the fiber is intermediate between that predicted by the fast- and slow-diffusion models and that on the time-scale of the experiment the equilibration of the nucleotide between the fiber and the surrounding medium may not be complete. This effect of diffusion needs to be considered when results of experiments carried out with fibers held in an aqueous medium are compared with results obtained for fibers held in oil or in air.

We also considered other variables in the model. The time course of relaxation depends on the caged ATP species used, with relaxation after photolytic release of ATP from DMB-caged ATP being faster than from NPE-caged ATP (Fig. 6 *a*). The slower relaxation predicted when using NPE-caged ATP is reflected in our data. Another aspect of the model that was considered concerned whether states DA and DS were, like LD, cooperative in promoting re-attachment. Re-attachment in DA and DS markedly prolonged the tension plateau and delayed relaxation. We cannot rule out this possibility in view of the threshold effect in the tension decline described above, but we consider it unlikely.

Models of muscular contraction such as that proposed by Botts et al. (1973) depend on the relationship between pairs of adjacent cross-bridges. Besides the examples already quoted, the link between complex tension responses and cross-bridge interactions with bound nucleotide have been suggested previously (Horiuti et al., 1991; Schoenberg, 1993 and references therein; Shimizu et al., 1992). The data and model presented here focus attention on the particular role of bound ADP in promoting cross-bridge cooperativity.

CONCLUSION

The results indicate that some form of cooperative behavior is required to explain the transient rise in force sometimes observed during relaxation of muscle fibers from the rigor state by photolysis of caged ATP. We demonstrate that the presence of ADP in the rigor muscle fiber accentuates such cooperativity.

P_i does not affect the time course of relaxation in apyrase-treated fibers in the absence of added ADP. This supports the view that cooperative cross-bridge re-attachments do not occur unless ADP is present.

A model is described in which the cooperative behavior arises between pairs of cross-bridges. It is likely that more complicated but perhaps more realistic models would account for our observations more closely. For example, cooperativity may extend over a larger number of cross-

bridges, or cross-bridge behavior including threshold responses may be affected by tension. The model presented here requires that there is a difference in the behavior of the initial ADP-containing rigor cross-bridges compared with re-attached cross-bridges. These initial ADP-containing cross-bridges are responsible for the maintenance of thin filament activation during relaxation from rigor and may bear some resemblance to ADP-containing cross-bridges in smooth muscle responsible for the latch state.

REFERENCES

Blinks, J. R. 1965. Influence of osmotic strength on cross-section and volume of isolated single muscle fibres. *J. Physiol.* 177:42–57.

Botts, J., R. Cooke, C. Dos Remedios, J. Duke, R. Mendelson, M. F. Morales, T. Tokiwa, and G. Viniegra. 1973. Does a myosin cross-bridge progress arm-over-arm on the actin filament? *Cold Spring Harbor Symp. Quant. Biol.* 37:195–200.

Bremel, R. D., J. M. Murray, and A. Weber. 1973. Manifestations of cooperative behavior in the regulated actin filament during activated ATP hydrolysis in the presence of Ca^{++}. *Cold Spring Harbor Symp. Quant. Biol.* 37:267–276.

Bremel, R. D., and A. Weber. 1972. Co-operation within actin filaments in vertebrate skeletal muscle. *Nature New Biol.* 238:97–101.

Chase, P. B., and M. J. Kushmerick. 1988. Effects of pH on contraction of rabbit fast and slow muscle fibers. *Biophys. J.* 53:935–946.

Cooke, R., and E. Pate. 1985. The effects of ADP and phosphate on the contraction of muscle fibers. *Biophys. J.* 48:789–798.

Corrie, J. E. T., Y. Katayama, G. P. Reid, M. Anson, and D. R. Trentham. 1992. The development and application of photosensitive caged compounds to aid time-resolved structure determinations of macromolecules. *Phil. Trans. R. Soc. Lond. A.* 340:233–244.

Corrie, J. E. T., and D. R. Trentham. 1992. Synthetic, mechanistic and photochemical studies of phosphate esters of substituted benzoins. *J. Chem. Soc. Perkin Trans I.* 2409–2417.

Corrie, J. E. T., and D. R. Trentham. 1993. Caged nucleotides and neurotransmitters. *In* Biological Applications of Photochemical Switches. H. Morrison, editor. John Wiley & Sons, New York. 243–305.

Dantzig, J. A., Y. E. Goldman, M. L. Luttman, D. R. Trentham, and S. K. A. Woodward. 1989. Binding of caged-ATP diastereoisomers to rigor cross-bridges in glycerol-extracted fibres of rabbit psoas muscle. *J. Physiol.* 418:61P.

Dantzig, J. A., M. G. Hibberd, D. R. Trentham, and Y. E. Goldman. 1991. Cross-bridge kinetics in the presence of MgADP investigated by photolysis of caged ATP in rabbit psoas muscle fibres. *J. Physiol.* 432:639–680.

Eastwood, A. B., D. S. Wood, K. L. Bock, and M. M. Sorenson. 1979. Chemically skinned mammalian skeletal muscle. The structure of skinned rabbit psoas tissue. *Cell.* 11:553–566.

Ferenczi, M. A. 1986. Phosphate burst in permeable muscle fibers of the rabbit. *Biophys. J.* 50:471–477.

Ferenczi, M. A., Y. E. Goldman, and R. M. Simmons. 1984. The dependence of force and shortening velocity on substrate concentration in skinned muscle fibres from *Rana temporaria*. *J. Physiol.* 350:519–543.

Fuglsang, A., A. Khromov, K. Török, A. V. Somlyo, and A. P. Somlyo. 1993. Flash photolysis studies of relaxation and cross-bridge detachment: higher sensitivity of tonic than phasic smooth muscle to MgADP. *J. Muscle Res. Cell Motil.* 14:666–667.

Goldman, Y. E., M. G. Hibberd, J. A. McCray, and D. R. Trentham. 1982. Relaxation of muscle fibres by photolysis of caged ATP. *Nature.* 300:701–705.

Goldman, Y. E., M. G. Hibberd, and D. R. Trentham. 1984a. Relaxation

of rabbit psoas muscle fibres from rigor by photochemical generation of adenosine 5'-triphosphate. *J. Physiol.* 354:577–604.

Goldman, Y. E., M. G. Hibberd, and D. R. Trentham. 1984b. Initiation of active contraction by photogeneration of adenosine-5'-triphosphate in rabbit psoas muscle fibres. *J. Physiol.* 354:605–624.

Goldman, Y. E., and R. M. Simmons. 1984. Control of sarcomere length in skinned muscle fibres of *Rana temporaria* during mechanical transients. *J. Physiol.* 350:497–518.

Harnett, D. L. 1975. Introduction to Statistical Methods. Addison-Wesley, Reading, MA.

Horiuti K., T. Sakoda, and K. Yamada. 1993. Mechanical response to photolytic ATP pulses of skinned muscle fibres pre-activated with a small pulse of ATP. *J. Muscle Res. Cell Motil.* 14:335–340.

Houadjeto, M., F. Travers, and T. Barman. 1992. Ca^{2+}-activated myofibrillar ATPase: transient kinetics and the titration of its active sites. *Biochemistry.* 31:1564–1569.

Hibberd, M. G., J. A. Dantzig, D. R. Trentham, and Y. E. Goldman. 1985. Phosphate release and force generation in skeletal muscle fibers. *Science.* 228:1317–1319.

Hibberd, M. G., Y. E. Goldman, and D. R. Trentham. 1984. Laser-induced photogeneration of ATP: a new approach to the study of chemical kinetics of muscle contraction. *Curr. Top. Cell Regul.* 24:357–364.

Hoard, D. E., and D. G. Ott. 1965. Conversion of mono- and oligodeoxyribonucleotides to 5'-triphosphates. *J. Am. Chem. Soc.* 87:1785–1788.

Kawai, M., J. S. Wray, and Y. Zhao. 1993. The effect of lattice spacing change on cross-bridge kinetics in chemically skinned rabbit psoas muscle fibers. 1. Proportionality between the lattice spacing and fiber width. *Biophys. J.* 64:187–196.

Luo Y., R. Cooke, and E. Pate. 1993. A model of stress relaxation in cross-bridge systems: effect of a series elastic element. *Am. J. Physiol.* 265: C279–C288.

Martin, H., and R. J. Barsotti. 1991. Kinetics of cardiac muscle relaxation from rigor initiated by laser photolysis of caged ATP. *Biophys. J.* 59:417a. (Abstr.)

Martin, H., and R. J. Barsotti. 1994. Relaxation from rigor of skinned trabeculae of the guinea pig by laser flash photolysis of caged ATP. *Biophys. J.* 66:1115–1128.

Moisescu, B. G. 1976. Kinetics of reaction in calcium-activated skinned muscle fibres. *Nature.* 262:610–613.

Molnar, J., and L. Lorand. 1961. Studies on apyrases. *Arch. Biochem. Biophys.* 93:353–363.

Nishiye, E., A. V. Somlyo, K. Török, and A. P. Somlyo. 1993. The effects

of MgADP on cross-bridge kinetics: a laser flash photolysis study of guinea pig smooth muscle. *J. Physiol.* 460:247–271.

Peckham, M., M. A. Ferenczi, and M. Irving. 1994. A birefringence study of changes in myosin orientation during relaxation of skinned muscle fibers induced by photolytic ATP. *Biophys. J.* 67:1141–1148.

Poole, K. J. V., Y. Maèda, G. Rapp, and R. S. Goody. 1991. Dynamic x-ray diffraction measurements following photolytic relaxation and activation of skinned rabbit psoas fibres. *Adv. Biophys.* 27:63–75.

Rosenfeld, S. S., and E. W. Taylor. 1987a. The mechanism of regulation of actomyosin subfragment 1 ATPase. *J. Biol. Chem.* 262:9984–9993.

Rosenfeld, S. S., and E. W. Taylor. 1987b. The dissociation of 1-N^6-ethenoadenosine diphosphate from regulated actomyosin subfragment 1. *J. Biol. Chem.* 262:9994–9999.

Schoenberg, M. 1993. Equilibrium muscle crossbridge behavior: the interaction of myosin crossbridges with actin. *Adv. Biophys.* 29:55–73.

Shimizu, H., T. Fujita, and S. Ishiwata. 1992. Regulation of tension development by MgADP and Pi without Ca^{2+}. *Biophys. J.* 61: 1087–1098.

Sleep, J., and K. Burton. 1990. The use of apyrase in caged ATP experiments. *Biophys. J.* 57:542a. (Abstr.)

Thirlwell, H., F. Bancel, and M. A. Ferenczi. 1993a. Relaxation of rigor tension by photolysis of caged ATP in permeabilized muscle fibers of the rabbit *Biophys. J.* 64:251a. (Abstr.)

Thirlwell, H., G. P. Reid, J. E. T. Corrie, D. R. Trentham, and M. A. Ferenczi. 1993b. Tension responses in permeabilised muscle fibres of the rabbit following laser pulse photolysis of a new "caged ATP," the P^3-3',5'-dimethoxybenzoin ester of ATP. *J. Physiol.* 473:79P.

Thirlwell, H., J. A. Sleep, J. E. T. Corrie, D. R. Trentham, and M. A. Ferenczi. 1994. Inhibition of fiber shortening velocity by caged ATP compounds. *Biophys. J.* 66:302a. (Abstr.)

Trentham, D. R., J. E. T. Corrie, and G. P. Reid. 1992. A new caged ATP with rapid photolysis kinetics. *Biophys. J.* 61:295a. (Abstr.)

Walker, J. W., G. P. Reid, J. A. McCray, and D. R. Trentham. 1988. Photolabile 1-(2-nitrophenyl)ethyl phosphate esters of adenine nucleotide analogues. Synthesis and mechanism of photolysis. *J. Am. Chem. Soc.* 110:7170–7177.

Walker, J. W., G. P. Reid, and D. R. Trentham. 1989. Synthesis and properties of caged nucleotides. *Methods Enzymol.* 172:288–301.

Webb, M. R. 1992. A continuous spectrophotometric assay for inorganic phosphate and for measuring phosphate release kinetics in biological systems *Proc. Natl. Acad. Sci. USA.* 89:4884–4887.